Two-Dimensional Ising Model Criticality in a Three-Dimensional Uniaxial Relaxor Ferroelectric with Frozen Polar Nanoregions

Wolfgang Kleemann,[1,*] Jan Dec,[1,2] Vladimir V. Shvartsman,[1] Zdravko Kutnjak,[3] and Thomas Braun[1]

[1]*Angewandte Physik, Universität Duisburg-Essen, D 47048 Duisburg, Germany*
[2]*Institute of Physics, University of Silesia, PL 40-480 Katowice, Poland*
[3]*Jozef Stefan Institute, P.O. Box 3000, SV 1001 Ljubljana, Slovenia*

(Received 12 May 2006; published 10 August 2006)

The charge-disordered three-dimensional uniaxial relaxor ferroelectric $Sr_{0.61}Ba_{0.39}Nb_2O_6$ splits up into metastable polar nanoregions and paraelectric interfaces upon cooling from above T_c. The frozen polar nanoregions are verified by piezoresponse force microscopy, respond domainlike to dynamic light scattering and dielectric excitation, reveal nonergodicity at $T > T_c$ via global aging, and coalesce into polar nanodomains below T_c. Contrastingly, the percolating system of unperturbed interfaces becomes ferroelectric with two-dimensional Ising-model-like critical exponents $\alpha = 0$, $\beta = 1/8$, and $\gamma = 7/4$, as corroborated by ac calorimetry, second harmonic generation, and susceptometry, respectively.

DOI: 10.1103/PhysRevLett.97.065702 PACS numbers: 64.60.−i, 65.40.Ba, 68.37.Ps, 77.22.−d

Crystals and ceramics of the strontium-barium niobate family $Sr_xBa_{1-x}Nb_2O_6$ (SBN) with $0 < x < 1$ are important materials, e.g., for applications in sensors, actuators, and nonlinear optics [1]. Their spontaneous ferroelectric polarization P_s is a single component vector directed along the c direction, which drives the symmetry point group from paraelectric $4/mmm$ to polar 4 mm at the phase transition [2]. Since SBN lacks any optic soft mode [3], it can be mapped onto an order-disorder Ising-type pseudospin model with short-range interactions. Dipolar corrections to criticality are expected to be negligible [4] due to the limitation of the correlation length by intrinsic charge disorder. This is a consequence of random empty sites within the unfilled tungsten bronze structure [Fig. 1(a)]. They create quenched random electric fields (RFs) [5], which drive the system into the three-dimensional random-field Ising model (RFIM) universality class [6]. These conditions have recently been found to be fulfilled in congruently melting SBN with $x = 0.61$ (SBN61), which has been the very first materialization of the ferroic RFIM [4]. For this system, theory predicts the existence of a phase transition into long-range order for a small enough field strength with criticality controlled by a $T = 0$ fixed point [7] and preceded by giant critical slowing down above T_c [8]. For RFs exceeding a critical amplitude, the system breaks up into a domain state [9,10].

Since all of the experimental data on RFIM systems had hitherto been collected on dilute uniaxial antiferromagnets in an external magnetic field (DAFF) [7,11], the newly discovered ferroelectric RFIM system SBN was expected to shed some light on understanding the criticality of the 3D RFIM, whose exponents had been disputed all along [7]. However, contrary to the theoretically expected order parameter exponent [12] $\beta \approx 0$, NMR measurements on SBN revealed $\beta \approx 0.15 \pm 0.03$ [13], in close agreement with $\beta \approx 0.16 \pm 0.03$ observed on the DAFF system $Fe_{0.85}Zn_{0.15}F_2$ [14]. Logarithmic singularities of the specific heat, and, hence, critical exponents $\alpha \approx 0$, are found for both the nonferroic DAFF system $Fe_{0.93}Zn_{0.07}F_2$ [15] and the ferroic RFIM system SBN (this Letter), while theory predicts an exponent $\alpha \approx -0.5$ [11].

In this Letter, we suggest that the systematic misfit between experiment and theory is due to the appearance of a self-organized polar nanostructure in close vicinity above the critical temperature T_c. Its origin is related to the appearance of domain states in the RFIM below T_c [6,12]. As depicted in Fig. 1(a), quenched electric RFs in SBN arise from randomly distributed empty sites (equivalent to

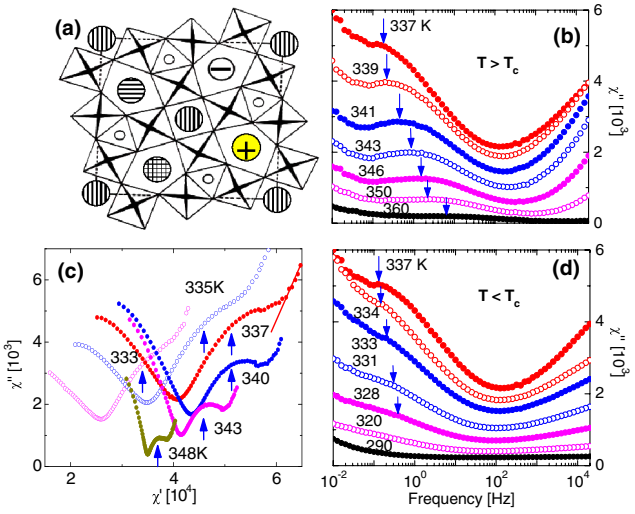

FIG. 1 (color online). (a) The basic octahedral framework of the tungsten bronze structure of $Sr_xBa_{1-x}Nb_2O_6$ with A_1 sites occupied by Sr^{2+} (vertically hatched), Ba^{2+} (horizontally hatched), Sr^{2+} or Ba^{2+} (checked), Ce^{3+} (excess charge +) or vacancy (−), octahedral B_1 sites occupied by Nb^{5+}. (b)–(d) Dielectric loss spectra χ'' vs f of SBN61 recorded at temperatures (b) above and (d) below $T_c = 337$ K and Cole-Cole plots χ'' vs χ' for $333 \leq T \leq 348$ K in (c). Relaxation anomalies of the PNRs are marked by vertical arrows. A straight line for $T = 337$ K denotes the proportionality $\chi'' \propto \chi' - \chi_\infty$ in (c).

negative excess charges). They are increased by trivalent dopants such as Ce^{3+} [positive excess charges, Fig. 1(a)]. Their mesoscopic fluctuations, i.e., the local statistical excess of either field component $+E_z$ or $-E_z$ ($\approx\sqrt{N}$ out of a cluster of N lattice sites in the case of a bimodal distribution of RFs) favors the alignment of polar clusters with polarization $+P_s$ or $-P_s$, respectively. These polar nanoregions (PNRs) are RF-stabilized against thermal agitation below the so-called Burns temperature T_d ($\approx$750 K in SBN61 [16]). The formation of PNRs is a common consequence of disorder in highly polarizable ferroelectric materials [17]. They are frozen on finite time scales and contribute to the giant polydispersivity of relaxors [18]. In the critical region $T \geq T_c$, they are expected to grow due to increased ferroelectric correlations. Their borders with the paraelectric environment are naturally defined by regions where the RFs form a quasistaggered electric field with very short correlation lengths of its fluctuations. The size distribution of the PNRs is expected to resemble that found for the frozen ferroelectric nanodomains below T_c, i.e., following an inverse power law with exponential cutoff [19].

Within this distribution, the largest (''mesoscopic'') PNRs have been visualized by piezoresponse force microscopy (PFM; Topometrix, Explorer). Figure 2 shows their evolution in SBN61:1.1% Ce^{3+} ($T_c = 320$ K) after establishing paraelectric disorder by annealing for 1 h at $T =$ 420 K. The PFM image at $T = 326$ K ($>T_c$) [Fig. 2(a)] resolves $+P_s$ (red = dark) and $-P_s$ (white) nanoregions with a typical diameter of $\approx$100 nm. They are separated by paraelectric (yellow = grey) interfaces, which are probably subdivided into smaller PNRs with narrower interfaces, which cannot be resolved against noise. On cooling to 295 K ($<T_c$), the interface thickness shrinks, while the PNRs slightly coarsen into nanodomains [19]. Figure 2(b) was taken after ''annealing'' for about 30 days, i.e., after reaching quasiequilibrium with nearly vanishing neutral interfaces. As a signature of the 3D RFIM domain state [12], ''nesting of frozen spin regions'' is observed. It should be noticed that the mesoscopic PNRs are reproducible at different instants and much longer lived than the PFM measurement times ($\approx 10^2$ s). Similarly robust ordered regions have recently been observed in the cubic relaxor ferroelectric $PbZn_{1/3}Nb_{2/3}O_3$ by diffuse x-ray scattering [20]. It is, hence, tempting to consider them as ordered subsystems of the polar solid, which thus reveals the properties of two distinct ''phases,'' frozen PNRs and ''controllable'' [12] interfaces.

This conjecture is verified by several signatures. First, ''critical opalescence''—unique for a solid—was recently [21] observed by dynamic light scattering (DLS) in a single crystal of SBN61:1.1 mol % Ce^{3+} ($T_c = 320$ K). It clearly indicates the spontaneous formation of polar clusters with giant photorefractive response. The observed change of dynamic behavior from a broad dispersion step above T_c to underdamped resonancelike Lorentz-shaped response

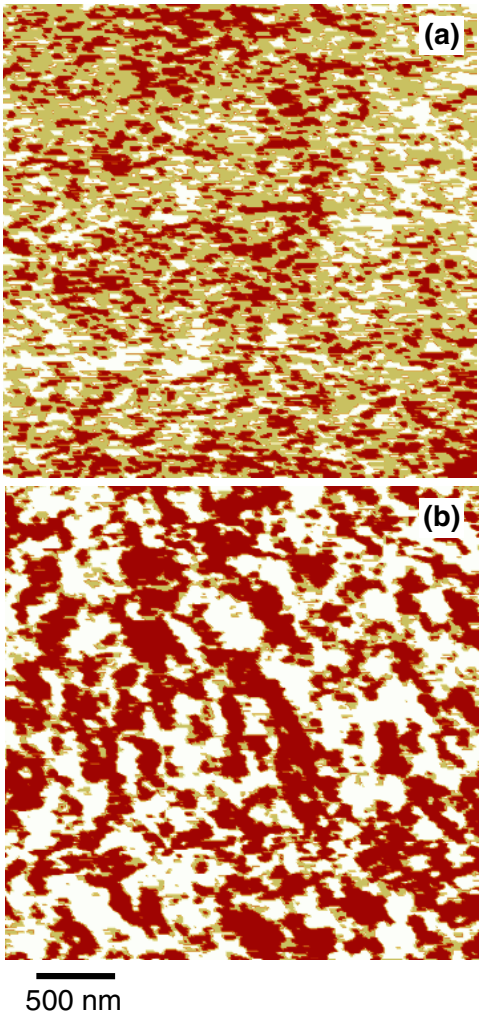

FIG. 2 (color online). Piezoresponse microscope images of SBN61:1.1 mol % Ce^{3+} viewed along the c axis (a) at $T =$ 326 K and (b) after 30 days isothermal annealing at $T = 295$ K. The color codes ''red = dark,'' ''white,'' and ''yellow = grey'' denote positive, negative, and vanishing local polarization, respectively.

below T_c confirms the observed change from isolated PNRs [Fig. 2(a)] to sharply contoured polar nanodomains [Fig. 2(b)], where the RF distribution even seems to provide weak restoring forces.

Second, excitation of the PNRs with electric ac fields yields a similar spectral response as the DLS structure factor [21]. The complex susceptibility $\chi' - i\chi''$ was measured on pure SBN61 ($T_c \approx 337$ K) within the frequency range $10^{-3} \leq f \leq 10^6$ Hz using a Solartron 1260 impedance analyzer with a 1296 dielectric interface. Below $T \approx$ 360 K, we observe [Fig. 1(b)] a broad peak in the dielectric loss spectra $\chi''(f)$ shifting from 10 to 0.1 Hz (arrows) and increasing in height when cooling towards T_c. At lower frequencies, the response continues as an inverse power law $\chi'' \propto f^{-s}$, with $s \approx 0.8$. Both features are more clearly seen in the Cole-Cole plots χ'' vs χ' in Fig. 1(c), where the peak transforms into a compressed semicircular anomaly

(arrows) and the low-f power law into a straight line $\chi'' \propto \chi' - \chi_\infty$, with slope $\tan\alpha = \pi s/2$ (indicated for $T = 337$ K). In analogy to similar spectra found for domain wall segmental relaxation and creep, respectively [22], we interpret the PNR response observed in SBN as being due to very low-frequency interface creep crossing over into "high"-frequency interfacial segment relaxation. Here the role of the domain walls involved in conventional spectra [22] is taken by the borders between the PNRs and the paraelectric interface, which is defined by the distribution of RFs. By analogy with the well-known Griffiths phase scenario of dilution-induced precursor transitions [23], one might attribute the mesoscopic fraction of PNRs to RF-induced local phase transitions as recently proposed for the DAFF system $Fe_{0.53}Zn_{0.47}F_2$ [24]. Within the interfaces shown in Figs. 2(a) and 2(b), there is room for PFM-invisible unfrozen small PNRs. They are assumed to give rise to the well-known [3] dielectric response at higher frequencies [$f > 10^2$ Hz in Fig. 1(b) and left-hand wings in Fig. 1(c)]. When cooling to below T_c, the PNR spectra finally fade out [Fig. 1(d), arrows] and transform into domain wall-induced creep and relaxation spectra [25]. The respective Cole-Cole plots in Fig. 1(c) reveal extreme broadening of the Debye-type semicircular anomalies due to increased polydispersivity of the remaining interfaces (arrows) and vanish below about 328 K. Obviously, the novel PNR response is restricted to the critical range of the system $|\varepsilon| < 0.06$, where $\varepsilon = T/T_c - 1$.

A third remarkable feature related to the PNR formation is the isothermal aging of the dielectric permittivity as shown in Fig. 3 (right-hand side). During a wait time of 67 h at $\varepsilon = 0.04$ (350 K) after cooling in zero external field

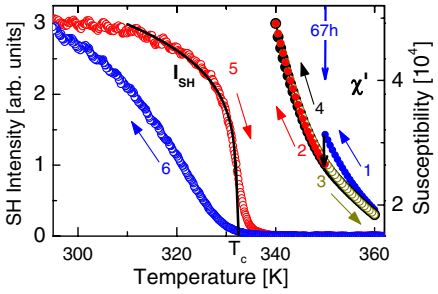

FIG. 3 (color online). Temperature dependences of the dielectric susceptibility χ' and of the second harmonic intensity I_{SH}. Right side: χ' vs T of SBN61 ($T_c = 337$ K) recorded at $f = 0.1$ Hz on cooling from $T = 360$ to 350 K (curve 1), isothermally annealing at 350 K for 67 h, further cooling to 340 K (curve 2), subsequent heating to 360 K (curve 3), and, again, cooling to 340 K (curve 4). Left side: I_{SH} vs T excited in an ac slab of SBN61:0.8 mol % Ce^{3+} ($T_c = 332$ K) by Nd:YAG laser light at $\lambda = 532$ nm in 180° geometry on heating after 24 h room temperature annealing (curve 5) and after subsequent slow cooling (curve 6). The periodic wiggles near room temperature are due to periodic phase mismatch induced by the temperature dependent linear birefringence of SBN. The solid black line denotes a best fit of curve 5 to the equation $I_{SH} \propto |\varepsilon|^{2\beta} + I_0$ (see text).

(curve 1), an irreversible drop of $\chi'(T)$ by about 15% occurs at a typical "PNR frequency" $f = 0.1$ Hz. Obviously, nonergodicity—unexpected in the paraelectric regime—is encountered. Inspection shows that the decrease of the dielectric susceptibility follows a stretched exponential decay law, which is typical of hierarchical growth processes. The "hardened" susceptibility (curve 2) is reproducible upon subsequent heating (curve 3) and cooling (curve 4). Absence of memory effects ("hole burning") verifies global equilibration while aging. This can be attributed to an irreversible growth of the mesoscopic PNRs while optimizing their local free energy gain, decreasing their total interface area, and, hence, decreasing χ' and χ''.

Let us finally consider critical behavior. The order parameter P_s vs T is conveniently measured via optical second harmonic (SH) generation excited by a pulsed Nd:YAG laser (Baasel, BLS 600). Its intensity I_{SH} is proportional to ${P_s}^2$ under phase-matched conditions or—as in the present case—for an incoherent multidomain state. The zero-field heating curve of an equilibrated sample of SBN61:0.8 mol % Ce^{3+} ($T_c = 332$ K), I_{SH} vs T, in Fig. 3 (curve 5) varies as $I_{SH} \propto |\varepsilon|^{2\beta} + I_0$ within the range $0.001 < |\varepsilon| < 0.06$ (solid line), where $T_c = 332.1 \pm 0.1$ K and $\beta = 0.13 \pm 0.02$ are best-fitted parameters. The errors account for slight systematic shifts of the parameters when varying the borders of the fitting range to within ±25%. Within errors, agreement is found with $\beta = 0.15 \pm 0.03$ obtained on SBN61 from ^{207}Nb NMR under similar conditions [13] and on the 3D DAFF $Fe_{0.85}Zn_{0.15}F_2$, $\beta = 0.16 \pm 0.02$ [14]. $I_0 \approx 0.05 I_{SH}(300\,\mathrm{K})$ is considered to be the noncritical contribution of the frozen PNRs. It should be mentioned that the zero-field cooling curve 6 in Fig. 3 fails to show criticality because of the extreme slowing down of the critical dynamics [8] despite extremely low cooling rates $dT/dt \approx -10$ mK/s.

Critical specific heat data were obtained by a computerized calorimeter [26] in the ac mode at an angular frequency $\omega = 0.077\ \mathrm{s}^{-1}$ and typical heating/cooling rates of 300 mK/h. Data obtained on SBN61:50 ppm Cr^{3+} ($T_c = 344$ K) after slow cooling in a poling field $E = 76.7$ kV/m (providing equilibrium close to long-range order) are shown in Fig. 4 (solid red symbols). They are excellently described together with a large noncritical lattice background within $0.001 < |\varepsilon| < 0.02$ by $C_p = A^{\pm}|\varepsilon|^{-\alpha} + B\varepsilon + C$, where $\alpha = -0.023 \pm 0.02$, $A^+ = -0.23$ J/g K, $A^- = -0.24$ J/g K, $B = 0.19$ J/g K, $C = 0.72$ J/g K, and $T_c = 344.33 \pm 0.05$ K (solid lines). Within errors, the cusplike anomaly (due to a very small negative value of α) is virtually undistinguishable from a logarithmic singularity ($\alpha = 0$), similarly as observed on the 3D DAFF system $Fe_{0.93}Zn_{0.07}F_2$ [15]. If the observed smearing of the C_p peak within $|\varepsilon| < 0.001$ is due to finite-size effects as discussed elsewhere [27] or hints at true asymptotic RFIM criticality predicted as a cusp with $\alpha \approx -0.5$ [12] remains an open issue. Much larger smearing due to extreme nonequilibrium, comparable to field-cooled

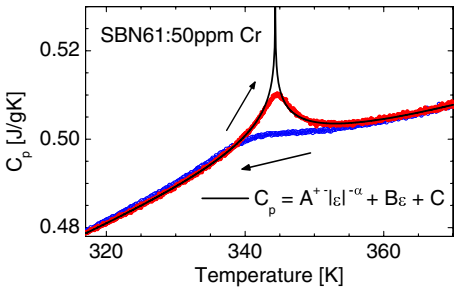

FIG. 4 (color online). Specific heat capacity of SBN:50 ppm Cr^{3+}, C_p vs T, measured with ac calorimetry at $\omega = 0.077\ s^{-1}$ on cooling in $E_z = 76.7\ kV/m$ (blue = light gray symbols) and on subsequent heating (red = dark gray symbols) fitted to $C_p = A^{\pm}|\varepsilon|^{-\alpha} + B\varepsilon + C$, with $T_c = 344.33 \pm 0.05$ K, $A^+ \approx A^-$, and $\alpha = -0.023 \pm 0.02$ (solid lines).

I_{SH} vs T in Fig. 3, is found when measuring C_p on field cooling (open blue symbols).

The present investigation has undoubtedly proved metastability, not only below but also *above* T_c. Aging of the paraelectric susceptibility (Fig. 3) obviously excludes true equilibrium criticality when approaching T_c. Extending the model of "*frozen*" and "*unfrozen*" (=field-controllable) regions considered in the RF controlled domain state [12] into the paraelectric regime, we argue that the mesoscopic PNRs must be considered frozen on finite time scales. On the other hand, the unfrozen interfaces can be considered as regions with very short-ranged correlations of the RFs, which are not able to select sizable polar clusters via their field energy gain. In these virtually 2D regions, which form a percolating network throughout the sample, a phase transition can take place under the constraint of a weakly disordering quasistaggered field. It merely shifts the ferroic T_c to somewhat lower temperatures as does the antiferroic Néel temperature in a homogeneous field. Being far from a multicritical point, the 2D Ising model criticality of the interface system, and, hence, $\alpha = 0$ [28] and $\beta = 0.125$ [29], will be preserved. It should be noticed that apart from these exponents the asymptotic susceptibility exponents of SBN61 $\gamma = 1.85 \pm 0.10$ [4] and $Fe_{0.93}Zn_{0.07}F_2$, $\gamma = 1.58 \pm 0.13$ [30] also agree within errors with that of the 2D Ising model $\gamma = 1.75$ [28]. Thus, the suspected [7] dimensional reduction of the RFIM from 3D to 2D is finally corroborated while discouraging further alternative attempts [31].

In conclusion, the obvious nonobservability of equilibrium RFIM criticality is a consequence of the extreme critical slowing down [8,11]. This applies also to DAFF systems, whose ground state is easily reached by zero-field cooling to below T_N and subsequent application of a homogeneous magnetic field [7,11]. Obviously, however, when approaching T_N under this field, the domain state unavoidably develops and hampers true critical behavior to be observed [14,15,30]. It appears challenging to verify the proposed crossovers between antiferromagnetic cluster freezing in DAFF systems, 2D Ising-type interfacial phase transition, and, finally—in the limit $t \to \infty$—true 3D RFIM criticality.

This work was supported by the Deutsche Forschungsgemeinschaft. We thank R. Pankrath, Universität Osnabrück, for providing the excellent samples of SBN61.

*Corresponding author.
Electronic address: kleemann@uni-duisburg.de

[1] Y. Xu, *Ferroelectric Materials and their Applications* (North-Holland, Amsterdam, 1991).
[2] J. R. Oliver, R. R. Neurgaonkar, and L. E. Cross, J. Appl. Phys. **64**, 37 (1988).
[3] E. Buixaderas *et al.*, J. Phys. Condens. Matter **17**, 653 (2005).
[4] W. Kleemann *et al.*, Europhys. Lett. **57**, 14 (2002).
[5] V. Westphal, W. Kleemann, and M. D. Glinchuk, Phys. Rev. Lett. **68**, 847 (1992).
[6] Y. Imry and S. K. Ma, Phys. Rev. Lett. **35**, 1399 (1975).
[7] D. P. Belanger and A. P. Young, J. Magn. Magn. Mater. **100**, 272 (1991).
[8] D. S. Fisher, Phys. Rev. Lett. **56**, 416 (1986).
[9] T. Schneider and E. Pytte, Phys. Rev. B **15**, 1519 (1977).
[10] B. E. Vugmeister, Ferroelectrics **120**, 133 (1991).
[11] A review of theoretical and experimental results on the critical behavior of various Ising models is given by D. P. Belanger, Braz. J. Phys. **30**, 682 (2000).
[12] A. A. Middleton and D. S. Fisher, Phys. Rev. B **65**, 134411 (2002).
[13] R. Blinc *et al.*, Phys. Rev. B **64**, 134109 (2001).
[14] F. Ye *et al.*, Phys. Rev. Lett. **89**, 157202 (2002).
[15] Z. Slanic and D. P. Belanger, J. Magn. Magn. Mater. **186**, 65 (1998).
[16] P. Lehnen, W. Kleemann, Th. Woike, and R. Pankrath, Eur. Phys. J. B **14**, 633 (2000).
[17] B. E. Vugmeister and H. Rabitz, Phys. Rev. B **57**, 7581 (1998).
[18] B. E. Vugmeister, Phys. Rev. B **73**, 174117 (2006).
[19] P. Lehnen, W. Kleemann, Th. Woike, and R. Pankrath, Phys. Rev. B **64**, 224109 (2001).
[20] G. Xu, Z. Zhong, Y. Bing, Z.-G. Ye, and G. Shirane, Nat. Mater. **5**, 134 (2006).
[21] W. Kleemann, P. Licinio, Th. Woike, and R. Pankrath, Phys. Rev. Lett. **86**, 6014 (2001).
[22] Th. Braun, W. Kleemann, J. Dec, and P. A. Thomas, Phys. Rev. Lett. **94**, 117601 (2005).
[23] R. B. Griffiths, Phys. Rev. Lett. **23**, 17 (1969).
[24] Ch. Binek, S. Kuttler, and W. Kleemann, Phys. Rev. Lett. **75**, 2412 (1995).
[25] W. Kleemann, J. Dec, S. Miga, Th. Woike, and R. Pankrath, Phys. Rev. B **65**, 220101(R) (2002).
[26] H. Yao, K. Ema, and C. W. Garland, Rev. Sci. Instrum. **69**, 172 (1998).
[27] Z. Kutnjak, S. Kralj, G. Lahajnar, and S. Zumer, Phys. Rev. E **68**, 021705 (2003).
[28] L. Onsager, Phys. Rev. **65**, 117 (1944).
[29] C. N. Yang, Phys. Rev. **85**, 808 (1952).
[30] Z. Slanic, D. P. Belanger, and J.-A. Fernandez-Baca, Phys. Rev. Lett. **82**, 426 (1999).
[31] J. F. Scott, J. Phys. Condens. Matter **18**, 7123 (2006).